Demyelinating Diseases: Myeloperoxidase as an Imaging Biomarker and Therapeutic Target[1]

Reza Forghani, MD, PhD
Gregory R. Wojtkiewicz, MS
Yinian Zhang, MD, PhD
Daniel Seeburg, MD, PhD
Benjamin R. M. Bautz, MA
Benjamin Pulli, MD
Andrew R. Milewski, BS
Wendy L. Atkinson, BS
Yoshiko Iwamoto, BS
Elizabeth R. Zhang, BS
Martin Etzrodt, MS
Elisenda Rodriguez, PhD
Clinton S. Robbins, PhD
Filip K. Swirski, PhD
Ralph Weissleder, MD, PhD
John W. Chen, MD, PhD

Purpose: To evaluate myeloperoxidase (MPO) as a newer therapeutic target and *bis*-5-hydroxytryptamide-diethylenetriaminepentaacetate-gadolinium (Gd) (MPO-Gd) as an imaging biomarker for demyelinating diseases such as multiple sclerosis (MS) by using experimental autoimmune encephalomyelitis (EAE), a murine model of MS.

Materials and Methods: Animal experiments were approved by the institutional animal care committee. EAE was induced in SJL mice by using proteolipid protein (PLP), and mice were treated with either 4-aminobenzoic acid hydrazide (ABAH), 40 mg/kg injected intraperitoneally, an irreversible inhibitor of MPO, or saline as control, and followed up to day 40 after induction. In another group of SJL mice, induction was performed without PLP as shams. The mice were imaged by using MPO-Gd to track changes in MPO activity noninvasively. Imaging results were corroborated by enzymatic assays, flow cytometry, and histopathologic analyses. Significance was computed by using the *t* test or Mann-Whitney *U* test.

Results: There was a 2.5-fold increase in myeloid cell infiltration in the brain ($P = .026$), with a concomitant increase in brain MPO level ($P = .0087$). Inhibiting MPO activity with ABAH resulted in decrease in MPO-Gd–positive lesion volume ($P = .012$), number ($P = .009$), and enhancement intensity ($P = .03$) at MR imaging, reflecting lower local MPO activity ($P = .03$), compared with controls. MPO inhibition was accompanied by decreased demyelination ($P = .01$) and lower inflammatory cell recruitment in the brain ($P < .0001$), suggesting a central MPO role in inflammatory demyelination. Clinically, MPO inhibition significantly reduced the severity of clinical symptoms ($P = .0001$) and improved survival ($P = .0051$) in mice with EAE.

Conclusion: MPO may be a key mediator of myeloid inflammation and tissue damage in EAE. Therefore, MPO could represent a promising therapeutic target, as well as an imaging biomarker, for demyelinating diseases and potentially for other diseases in which MPO is implicated.

Supplemental material: *http://radiology.rsna.org/lookup/suppl/doi:10.1148/radiol.12111593/-/DC1*

[1] From the Center for Systems Biology, Massachusetts General Hospital, Harvard Medical School, Richard B. Simches Research Center, 185 Cambridge St, Suite 5.210, Boston, MA 02114 (R.F., G.R.W., Y.Z., D.S., B.R.M.B., B.P., A.R.M., W.L.A., Y.I., E.R.Z., M.E., E.R., C.S.R., F.K.S., R.W., J.W.C.); Division of Neuroradiology, Department of Radiology, Massachusetts General Hospital, Harvard Medical School, Boston, Mass (R.F., J.W.C.); and Sir Mortimer B. Davis Jewish General Hospital and McGill University, Montreal, Quebec, Canada (R.F.). From the 2009 RSNA Annual Meeting. Received July 28, 2011; revision requested September 12; final revision received October 4; accepted October 18; final version accepted November 14. Supported in part by grants from the Dana Foundation and Department of Defense (W81WH-10-1-0694). R.F. received an RSNA Research Fellow Grant. E.R. supported by a Marie Curie Fellowship. Y.Z. supported by Shanghai Jiao Tong University School of Medicine. **Address correspondence to** J.W.C. (e-mail: *jwchen@mgh.harvard.edu*).

Activated circulating monocytes, macrophages, and microglia in the central nervous system can secrete a variety of enzymes and factors that result in breakdown of myelin proteins, presentation of antigens to T and B lymphocytes, and generation of high oxidative stress, all of which may contribute to myelin and axonal damage (1–6). Furthermore, while lymphocytes are most abundant during acute disease, microglial activation is present both in the acute and chronic phases (7) and can cause tissue damage despite a paucity of T cells in plaques in the chronic phase (7–9). Nonetheless, the currently approved immunomodulatory therapies for multiple sclerosis (MS) primarily target the lymphocytic response (10–15). The innate immune axis of inflammation remains mostly unaffected or only indirectly affected by currently available drugs. Therefore, modulation of potentially deleterious inflammatory enzymes secreted by recruited macrophages and tissue resident microglia is a relatively unexplored area for treatment of demyelinating diseases such as MS.

Myeloperoxidase (MPO) is one of the most abundant enzymes secreted by activated inflammatory cells (16) and is produced by monocytes, macrophages, microglia, and neutrophils. It is found at high levels in active human MS plaques (1,17). MPO generates highly reactive molecular moieties such as hypochlorite, tyrosyl radicals, and aldehydes that can covalently modify lipids, causing further local tissue damage and further perpetuating the inflammatory cascade (18,19). MPO can also promote endothelial dysfunction (20), upregulate inducible nitric oxide synthase that can exacerbate inflammation (21), and result in carbamylation of lipoproteins, leading to functional impairment (22). Thus, MPO may be an attractive target for both understanding and treating MS. However, although researchers in a number of investigations have tried to elucidate the role of MPO in MS, as well as in animal models of demyelinating disease, the role of MPO in inflammatory demyelination or as a potential therapeutic target remains unclear (17,23–27).

In this study, we hypothesize that blocking MPO activity in demyelinating diseases could be beneficial, resulting in decreased neuroinflammation and demyelination, and that the changes can be tracked in vivo by the activatable molecular magnetic resonance (MR) imaging agent *bis*-5-hydroxytryptamide-diethylenetriaminepentaacetate-gadolinium (Gd) (MPO-Gd) (28,29) that targets MPO activity. By using experimental autoimmune encephalomyelitis (EAE), a murine model of MS, we aimed to evaluate MPO-Gd as an imaging biomarker and MPO as a newer therapeutic target for demyelinating diseases such as MS.

Advances in Knowledge

- Inhibiting myeloperoxidase (MPO) activity resulted in decreased immune cell recruitment and demyelination in a mouse model of multiple sclerosis (MS).
- Blocking MPO activity improved symptoms and decreased mortality in a mouse model of MS, suggesting that MPO may represent a useful therapeutic target for MS.
- Changes in MPO can be accurately tracked with molecular imaging as a potential imaging biomarker for neuroinflammation.

Materials and Methods

EAE Induction, Treatment Protocol, and Clinical Scoring

The protocol for animal experiments was approved by the institutional animal care committee. EAE was induced in female SJL mice 6–10 weeks old (National Cancer Institute, Frederick, Md) with synthetic proteolipid protein (PLP139–151; Axxora, San Diego, Calif), as previously described (28) and described in additional detail in Appendix E1 (online). A total of 118 SJL mice were used for this study. We induced EAE in a total of 106 SJL mice and divided them into saline control (n = 47) and treated (n = 59) groups. Twelve additional sham mice were induced with identical steps except that proteolipid protein was not used.

4-Aminobenzoic acid hydrazide (ABAH) (Sigma-Aldrich, St Louis, Mo) is a specific irreversible (suicide) inhibitor for MPO (30,31). ABAH inhibits both the chlorination and peroxidation activities of MPO but does not inhibit other enzymes involved in H_2O_2 metabolism such as catalase or glutathione peroxidase and does not affect neutrophil degranulation (30,31). ABAH becomes more potent under inflammatory conditions where oxygen is rapidly consumed to generate hydrogen peroxide by nicotinamide adenine dinucleotide phosphate oxidase (31). ABAH is currently the most potent and specific inhibitor for MPO (32). To confirm the inhibitory effect of ABAH on

Published online before print
10.1148/radiol.12111593 **Content code:** BQ

Radiology 2012; 263:451–460

Abbreviations:
ABAH = 4-aminobenzoic acid hydrazide
EAE = experimental autoimmune encephalomyelitis
Gd = gadolinium
LAR = lesion activation ratio
MPO = myeloperoxidase
MS = multiple sclerosis
PBS = phosphate-buffered saline

Author contributions:
Guarantors of integrity of entire study, R.F., G.R.W., W.L.A., E.R.Z., J.W.C.; study concepts/study design or data acquisition or data analysis/interpretation, all authors; manuscript drafting or manuscript revision for important intellectual content, all authors; approval of final version of submitted manuscript, all authors; literature research, R.F., G.R.W., Y.Z., B.R.M.B., B.P., A.R.M., E.R.Z., J.W.C.; experimental studies, R.F., G.R.W., Y.Z., B.R.M.B., B.P., A.R.M., W.L.A., Y.I., E.R.Z., M.E., E.R., C.S.R., F.K.S., J.W.C.; statistical analysis, R.F., G.R.W., Y.Z., D.S., B.P., A.R.M., J.W.C.; and manuscript editing, R.F., G.R.W., Y.Z., B.P., A.R.M., W.L.A., Y.I., F.K.S., R.W., J.W.C.

Funding:
This research was supported by the National Institutes of Health (grants K08 HL081170, R01-NS070835, and R01-NS072167).

Potential conflicts of interest are listed at the end of this article.

MPO activity, we performed in vitro titration assays with different amounts of human MPO (Lee Biosolutions, St Louis, Mo) at fixed doses of ABAH (Fig E1 [online]). The resultant data were fitted to the following equation: $Y = B + (T - B)/\{1 + 10 \wedge [(X - \log IC_{50})]\}$, where B is bottom, T is top, and IC_{50} is 50% inhibitory concentration, to obtain the 50% inhibitory concentration of ABAH against MPO activity, using software (GraphPad Prism; GraphPad Software, La Jolla, Calif). Under our conditions, we found a 50% inhibitory concentration of 1.6 μmol/L ± 0.03 (standard error), which is similar to the literature value of 2.2 μmol/L (30).

To determine an effective treatment dose in vivo, we designed the trials to use doses of 20 mg/kg (n = 5), 40 mg/kg (n = 10 initially, with additional mice tested at this dosage later for a total of 45, as described below), and 80 mg/kg (n = 9) injected intraperitoneally (Appendix E1 [online]). Because ABAH is a small molecule with likely a short blood half-life, we treated mice twice a day. The 40 mg/kg regimen was found to be most clinically effective, whereas the 20 mg/kg dose was found to be ineffective and the 80 mg/kg regimen did not confer additional benefit compared with the 40 mg/kg dose (Fig E2 [online]). After establishing the treatment dosage, all mice were treated with 400 μL of saline (controls, n = 47) or 400 μL of ABAH at a dose of 40 mg/kg (n = 45), twice daily. Subsets of these mice were also used for imaging, biochemical, and histopathologic experiments, described below. Clinical assessment for disease activity was performed by using the standard five-point staging system for EAE. Additional detail is provided in Appendix E1 (online).

Isolation of Brain Inflammatory Cells and Flow Cytometry

Flow cytometry was used to evaluate for inflammatory cell infiltration of the brain in sham mice (n = 7) and in ABAH-treated (n = 10) and control (n = 17) mice with EAE. The data were evaluated by three authors (Y.Z., C.S.R., and F.K.S., each with more than 3 years of experience in immunologic analyses) in consensus. For isolation of inflammatory cells, mice were transcardially perfused with ice-cold phosphate-buffered saline (PBS) until colorless fluid appeared from the inferior cava. Extracted brains were stored in ice-cold Hanks' balanced salt solution, containing 15 mmol/L HEPES (*N*-2-hydroxyethylpiperazine-*N*'-2-ethanesulfonic acid) and 0.5% glucose. Brain tissue was mechanically ground in a glass tissue homogenizer in 3 mL of ice-cold Hanks' balanced salt solution. After homogenization, the cell suspension was filtered through a 40-μm cell strainer (BD Biosciences, San Jose, Calif) into 50-mL conical tubes and washed with 17 mL Hanks' balanced salt solution in a glass homogenizer. Finally, cells were formed into pellets at 1000*g* for 10 minutes at 4°C and resuspended in 4 mL ice-cold 75% Percoll (17-0891-01; GE Healthcare, Boston, Mass) (33). The resultant cell suspension was transferred to a 15-mL conical tube, gently layered with 5 mL ice-cold 25% Percoll and 4 mL ice-cold PBS. The density gradient was centrifuged in a swinging bucket rotor (Centrifuge 5810R; Eppendorf, Hamburg, Germany) at 800*g* for 25 minutes at 4°C. After centrifugation, a thick myelin-containing layer at the 0/25 Percoll-PBS interface was removed, and the cells at the 25/75 interface were collected. The suspension was then diluted at least threefold with ice-cold PBS, centrifuged at 1000*g* for 10 minutes at 4°C, and resuspended by using 1 mL staining buffer (1% fetal bovine serum and 0.5% bovine serum albumin in Dulbecco's PBS). The cells were then counted and stained for flow cytometry.

The following antibodies were used for flow cytometry: anti-CD90-PE, 53–2.1 (BD Biosciences); anti-NK1.1-PE, PK136 (BD Biosciences); anti B220-PE, RA3–6B2 (BD Biosciences); anti-CD49b-PE, DX5 (BD Biosciences); anti-Ly-6G-PE, IA8 (BD Biosciences); anti-CD45.2-APC, 104 (BD Biosciences); anti-CD11b-APC-Cy7, M1/70 (BD Biosciences); anti-Ly-6C-FITC, AL-21 (BD Biosciences); anti-F4/80-Biotin, C1:A3–1 (BioLegend, San Diego, Calif); anti-IA^b-Biotin, AF6–120.1 (BD Biosciences); and anti-CD11c-Biotin, HL3 (BD Biosciences).

Streptavidin–peridininchlorophyll protein (Streptavidin-PerCP; BD Biosciences) was used to label biotinylated antibodies. All myeloid cells were identified as CD45.1 + CD11b + cells. Monocytes and macrophages were identified as $CD11b^{high}$(B220/CD90/CD49b/NK1.1/Ly-6G)^{low}. Neutrophils were identified as $CD11b^{high}$ (B220/CD90/CD49b/NK1.1/Ly-6G)^{high}(F4/80/IA^b/CD11c)^{low} Ly-$6C^{int}$. The cell numbers of different cell populations were calculated as total cells multiplied by the percentage within the respective cell population gate. Data were acquired on a flow cytometer (LSR II; BD Biosciences) and analyzed with software (FlowJo 887; Tree Star, Ashland, Ore). To evaluate the inflammatory cell infiltration specific to EAE, mice with EAE were compared with sham mice. The effects of ABAH inhibition on cell recruitment were evaluated by comparing ABAH-treated mice with EAE with control (saline-treated) mice with EAE.

Western Blot and Peroxidase Assays

Freshly dissected brain tissue extracts were used for Western blot analysis and peroxidase assays (34). Western blots were performed and evaluated by one author (D.S., with 10 years of experience interpreting Western blots) to confirm the presence of MPO protein in the brain and to obtain a semiquantitative comparison of MPO protein in sham mice (n = 5) and mice with EAE (n = 6). Peroxidase activity assays were performed and evaluated in consensus by two authors (R.F. and Y.Z., each with more than 3 years of experience in enzyme analyses) to confirm enzymatic activity and corroborate imaging findings in ABAH-treated mice (n = 9) and saline control mice (n = 11) with EAE. Because we were primarily interested in secreted, active MPO, separate intracellular and extracellular extracts were obtained for peroxidase activity assays, modifying methods that were originally developed for goldfish (35). Additional information on tissue preparation and assays is described in detail in Appendix E1 (online).

MPO-Gd Molecular MR Imaging

To confirm the presence of MPO activity within inflammatory brain plaques in vivo and to evaluate the effects of MPO inhibition noninvasively in living animals, we performed MPO-Gd (*bis*-5-hydroxytryptamide-diethylenetriaminepentaacetate-gadolinium) molecular MR imaging in mice with EAE on day 10 after induction, at the time of early acute disease onset, with and without ABAH (n = 10 per group). MPO-Gd is an activatable MR imaging agent that reports *extracellular* MPO activity in vivo with high specificity and sensitivity (28,36). We did not delay imaging to the time of peak clinical illness between days 13 and 15 because lesion load at imaging can precede clinical illness (28), and at the time of peak clinical illness the blood-brain barrier breakdown and detectable lesion load may already be on the decline and potentially misrepresentative. Furthermore, not all mice survive to days 13–15, particularly in the control group, which would introduce a bias toward healthier mice in that group if evaluated at a time when sicker mice have died. In addition to revealing the burden of MPO-positive plaques, the degree of MPO-Gd enhancement is also a marker for oxidative stress in vivo (37), since the catalytic activation of the MPO-Gd agent results in oxidation of 5-hydroxytryptamide moieties.

The MPO-sensing MR imaging agent MPO-Gd was synthesized in our laboratory as previously described (29) and as described in Appendix E1 (online). Additional information about MPO-Gd, including mechanism of activation, pharmacokinetics, blood half-life, specificity, and cytotoxicity are also provided in Appendix E1 (online). MR imaging was performed by using an animal 4.7-T MR imaging unit (Bruker, Billerica, Mass) consisting of mouse coronal T2-weighted images and T1-weighted images obtained before and after intravenous administration of MPO-Gd (0.3 mmol/kg). In vivo MPO activation was determined by calculating the lesion activation ratio (LAR) on the basis of contrast-to-noise ratios of lesions on delayed (60 minutes) and early (6 minutes) contrast material–enhanced images, because early enhancement (6 minutes after contrast agent injection) represents mostly leakage through blood-brain barrier breakdown, whereas delayed enhancement is derived mostly from agent retention caused by MPO activation. An LAR of 1.8 or greater was considered to represent MPO-specific activity (28,29). MR images were independently evaluated by two authors (R.F. and J.W.C., each with more than 10 years of experience in interpreting MR images). Total lesion volume, total lesion count, average lesion enhancement intensity, as well as the total lesion enhancement intensity–area product (the sum total of the LAR of each lesion multiplied by the cross-sectional area of that lesion) were calculated. Additional detail on these calculations is provided in Appendix E1 (online).

Histopathologic Analysis

Histopathologic analysis was performed to assess for demyelination and inflammatory cell infiltration of the brains of control (saline-treated) and ABAH-treated mice with EAE. Fresh-frozen 5-μm brain sections were used. Demyelination was detected by using the Luxol fast blue–cresyl echt violet stain kit (DBS, Pleasanton, Calif). Sections were also examined for the presence of MPO by using MPO Ab-1 (NeoMarkers, Fremont, Calif) and for CD11b-positive cells by using a rat antimouse CD11b antibody (BD Biosciences). Analyses were independently performed by two authors (W.L.A. and A.R.M., each with more than 3 years of experience in interpreting these images). Details on the protocol and quantification are in Appendix E1 (online).

Statistical Analysis

Results were reported as mean ± standard error of measurement. The data were tested for normality by using the D'Agostino-Pearson normality test and for equality of variances by using the F test. If normality and equality of variances were not rejected at the .05 significance level, the group means were compared by using the t test. Otherwise, for nonnormally distributed data and/or the data with unequal variances, we used the nonparametric Mann-Whitney U test (flow cytometry comparing sham mice with mice with EAE, Western blot, and Luxol fast blue histopathologic quantification analyses). For survival analysis, the log-rank test was used. A P value less than .05 was considered to indicate a significant difference. When multiple samples were used for each animal, we first averaged all the samples for each animal to generate a single value before pooling the data for analysis. We used software for statistical analysis (GraphPad Prism 5; GraphPad Software).

Results

EAE Increases Myeloid Cell Recruitment and MPO Activity in the Brain

During acute active disease (day 10 after induction), by using flow cytometry, we found elevated myeloid cells (CD11b positive) in the brains of mice with EAE (Fig 1a). Compared with sham mice, there was a 2.5-fold increase in myeloid cells (5.3 ± 2.0, sham mice, n = 7; 13.4 ± 2.2, mice with EAE, n = 17; P = .026). Histologically, the cellular infiltrate appeared similar to that in human disease, with macrophages and microglia (CD11b positive) present (Fig 1b). Concomitant with the increase in brain myeloid cell infiltration on day 10, there was increased MPO protein in brains of mice with EAE compared with sham mice with Western blot analysis (100.0 ± 33.8, sham mice, n = 5; 741.3 ± 207.4, mice with EAE, n = 6; P = .0087) (Fig E3 [online]). There were widespread MPO-specific enhancing lesions in the brains of saline-treated mice with EAE at the time of acute active disease (Fig 2), whereas no such lesions were detectable in healthy or sham mice (28). Furthermore, MPO-specific enhancing lesions were also seen during relapses in mice with EAE (Fig E4 [online]), confirming continued elevated MPO activity during the chronic relapsing phase of the disease.

MPO-positive Plaques, Oxidative Stress, and Brain Leukocyte Infiltration Are Reduced after MPO Inhibition

Compared with saline-treated control mice with EAE, there was significantly reduced MPO-specific enhancing lesion volume (14.6 mm^3 ± 6.5, treated mice, n = 10; 41.8 mm^3 ± 9.1, controls, n = 10; P = .012) and lesion number (7.1 ± 2.1, treated mice; 19.0 ± 4.0, controls; P = .009) in mice given the irreversible MPO inhibitor ABAH (Fig 2a, 2c, 2d; Fig E1 [online]), consistent with a decrease in disease burden. Appendix E1 (online) provides the dose information. In addition, lesion enhancement intensity was lower in treated mice both at gross inspection (Fig 2b) and quantitatively by measuring MPO-specific LAR (2.9 ± 0.6, treated mice; 4.9 ± 0.9, controls; P = .03) (Fig 2e), revealing decreased oxidative activation of the molecular imaging agent. This represents a reduction of 41% in the activation of MPO-Gd with treatment. Because measurements of lesion enhancement intensity in isolation do not take into account lesion size, the total intensity-area product was also calculated and was likewise significantly lower in the ABAH-treated group (92 units · mm^2 ± 41.0, treated mice; 292 units · mm^2 ± 73.1, controls; P = .01) (Fig 2f).

Similar to the imaging findings, there was a 36% reduction in extracellular peroxidase activity in treated mice compared with controls (normalized activity, 100 ± 16, treated mice, n = 11; 64 ± 7, controls, n = 9; P = .03) (Fig 3a), but no significant difference was found in the intracellular fractions between the two groups (normalized activity, 100 ± 10, treated mice; 98 ± 12, controls; P = .44) (Fig 3b).

With the use of flow cytometry, we found a 35% decrease in the number of leukocytes recruited to the brain in ABAH-treated mice with EAE compared with saline-treated control mice with EAE (4.2×10^6 ± 0.23, treated mice, n = 10; 6.5×10^6 ± 0.37, controls, n = 10; $P < .0001$) (Fig 3c). Both myeloid (1.9×10^6 ± 0.13, treated mice; 3.3×10^6 ± 0.35, controls; P = .0016) and lymphoid (0.69×10^6 ± 0.11, treated mice; 1.1×10^6 ± 0.059, controls; P = .0081) cells were reduced by a similar amount (Fig 3c), consistent with a general reduction in inflammation by blocking MPO activity.

Figure 1

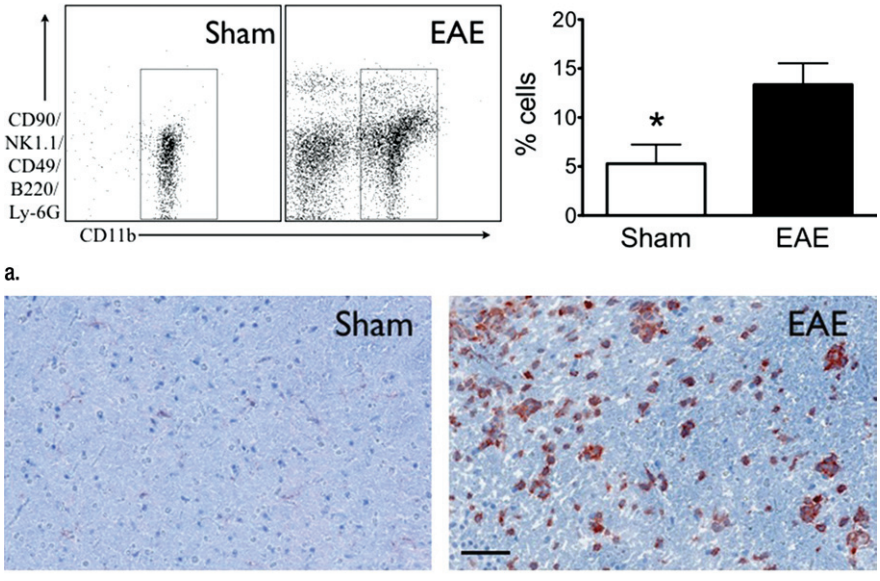

Figure 1: Increase in myeloid cells in brains of mice with EAE. **(a)** Left: Analysis from flow cytometry data shows a greater than twofold increase in myeloid cells in the brains of mice with EAE (n = 17) induced with proteolipid protein compared with sham control mice (n = 7). Right: Representative flow cytometry plots. * = $P < .05$. Error bars = standard error. **(b)** Representative immunohistochemical sections demonstrate markedly increased number of CD11b-positive cells in the brain of mice with EAE but not in the brain of sham control mice. Bar = 50 μm. (CD11b stain; original magnification, ×400.)

MPO Inhibition Decreases Tissue Damage and Demyelination in Mice with EAE and Improves Clinical Outcome

There was significantly less demyelination in ABAH-treated mice with EAE compared with saline-treated control mice with EAE (3.8 ± 0.7, ABAH-treated mice, n = 3; 8.0 ± 0.9, controls, n = 3; total sections evaluated, 27; P = .01) (Fig 4). Despite the presence of MPO-positive cells, in many areas there was much less demyelination in the ABAH-treated mice with EAE (Fig 4a, 4b), as evidenced by comparing top with bottom images.

We performed trials using 20 mg/kg, 40 mg/kg, and 80 mg/kg doses (Fig E2 [online], Appendix E1 [online]). We found 40 mg/kg to be the lowest effective dose. Therefore, we treated mice with either saline (control) or ABAH at a dose of 40 mg/kg administered intraperitoneally twice a day, and we followed up the mice to day 40 after induction. In the saline-treated group, clinical symptoms typically became apparent between days 9 and 11 and peaked between days 13 and 15 (acute exacerbation), with a relapse (first relapse) between days 20 and 30 after induction (Fig 5a, 5b, Fig E2 [online]). ABAH treatment significantly reduced the maximal clinical score during the acute exacerbation (ABAH-treated mice, 1.1 ± 0.4, n = 10; controls, 2.9 ± 0.4, n = 10; P = .0023) and first relapse (ABAH-treated mice, 1.2 ± 0.5, n = 10; controls, 3.5 ± 0.5, n = 8; P = .0025). Similarly, when the clinical data from additional mice with EAE from the above experiments were included, the total pooled clinical score during the first exacerbation was again significantly higher in controls compared with treated mice (controls, 2.1 ± 0.2, n = 45; ABAH-treated mice,

Figure 2

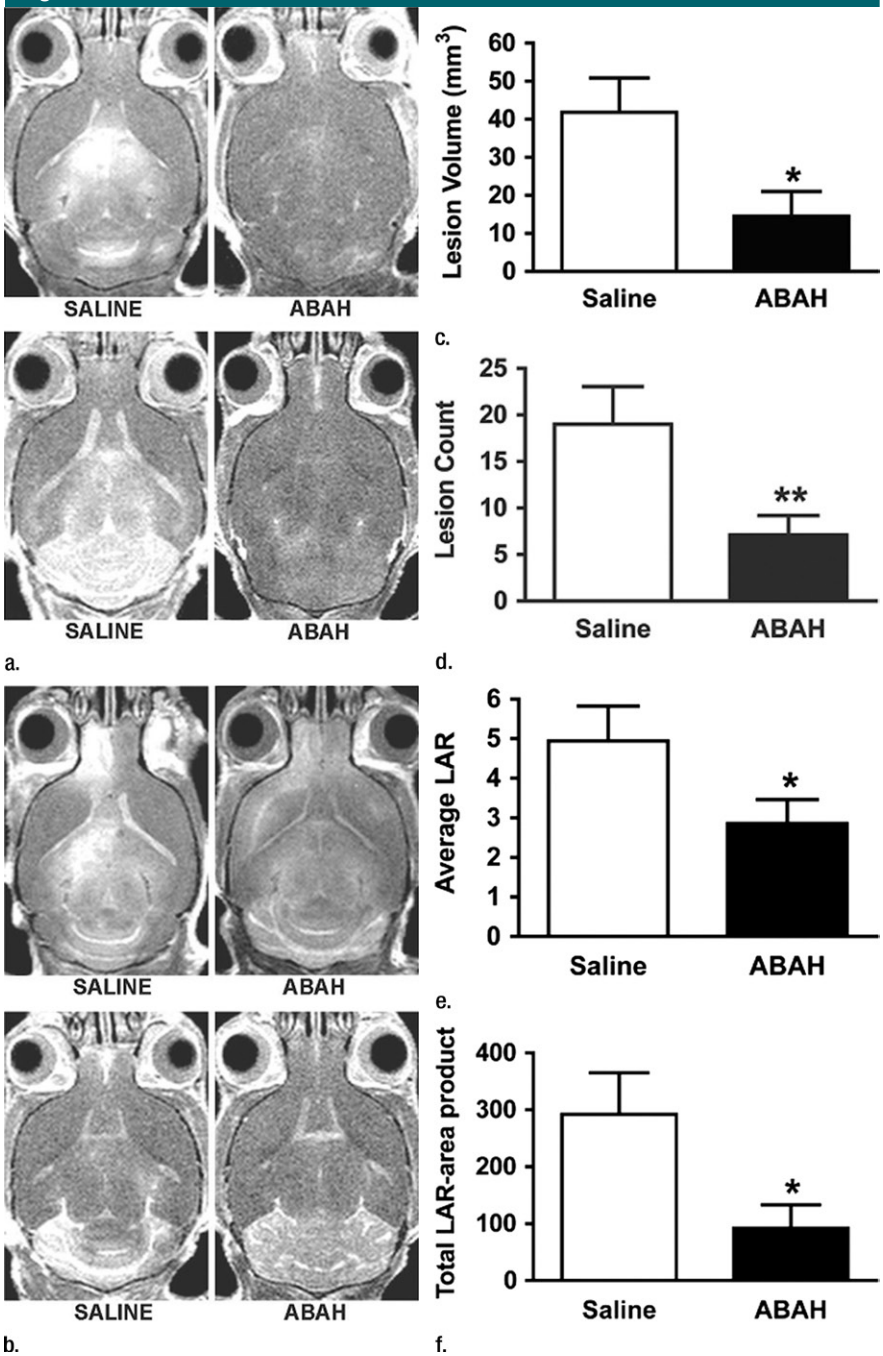

Figure 2: In vivo molecular MR imaging in mice with EAE. **(a)** Representative brain images demonstrate variable but extensive MPO-specific enhancing areas in the brains of mice with EAE that are decreased with MPO inhibition by using ABAH. **(b)** Images illustrate the changes to lesion enhancement intensity and were selected on the basis of similar lesion areas to compare the intensity of lesion enhancement, which is also markedly reduced in ABAH-treated mice with EAE compared with saline-treated mice with EAE. Each image represents the brain of a different mouse. Graphs show that the qualitative observations were confirmed quantitatively ($n = 10$ per group) with a significantly reduced MPO-specific **(c)** total lesion volume, **(d)** total lesion count, **(e)** LAR, and **(f)** total LAR-area product. $* = P < .05$, $** = P < .01$, error bars = standard error.

0.8 ± 0.2, $n = 45$; $P = .0001$) (Fig 5c). When we examined the mortality outcome of the treatment, ABAH treatment increased survival of mice with EAE, with only 30% (three of 10) of saline-treated control mice surviving to day 40, compared with 90% (nine of 10) of ABAH-treated mice surviving to day 40 ($P = .0051$) (Fig 5d). None of the ABAH-treated mice, regardless of dose, experienced adverse events not expected for mice with EAE.

Discussion

Despite emerging evidence suggesting that macrophages and microglia can directly contribute to tissue damage, the role of myeloid effector molecules and enzymes such as MPO in tissue damage and demyelination so far has not been well examined. In this study, we found that the MPO-specific inhibitor ABAH does not enter cells and that it inhibited only secreted extracellular MPO. We also confirm that changes in extracellular MPO activity can be accurately monitored in vivo with MPO-Gd molecular MR imaging. We found that inhibition of MPO activity resulted in decreased demyelination and tissue damage and inflammatory cell infiltration, with an improvement in clinical symptoms and mortality in EAE, a commonly used animal model for MS. Given the known association of inflammatory cell infiltration and demyelinating disease burden (2,3,7), this further suggests that MPO is an important mediator of tissue damage in inflammatory brain plaques. These observations reveal that MPO activity and associated oxidative stress are deleterious and constitute an important biochemical pathway underlying tissue damage in EAE.

Our current and other findings suggest that MPO activity is a potential biomarker for active inflammation and the consequent demyelination (28). As such, accurate, specific, and sensitive depiction of the in vivo MPO activity could be essential for evaluating the degree of active inflammation to monitor disease activity and guide therapy in demyelinating diseases. We previously demonstrated the in vitro and in vivo specificity

Figure 3

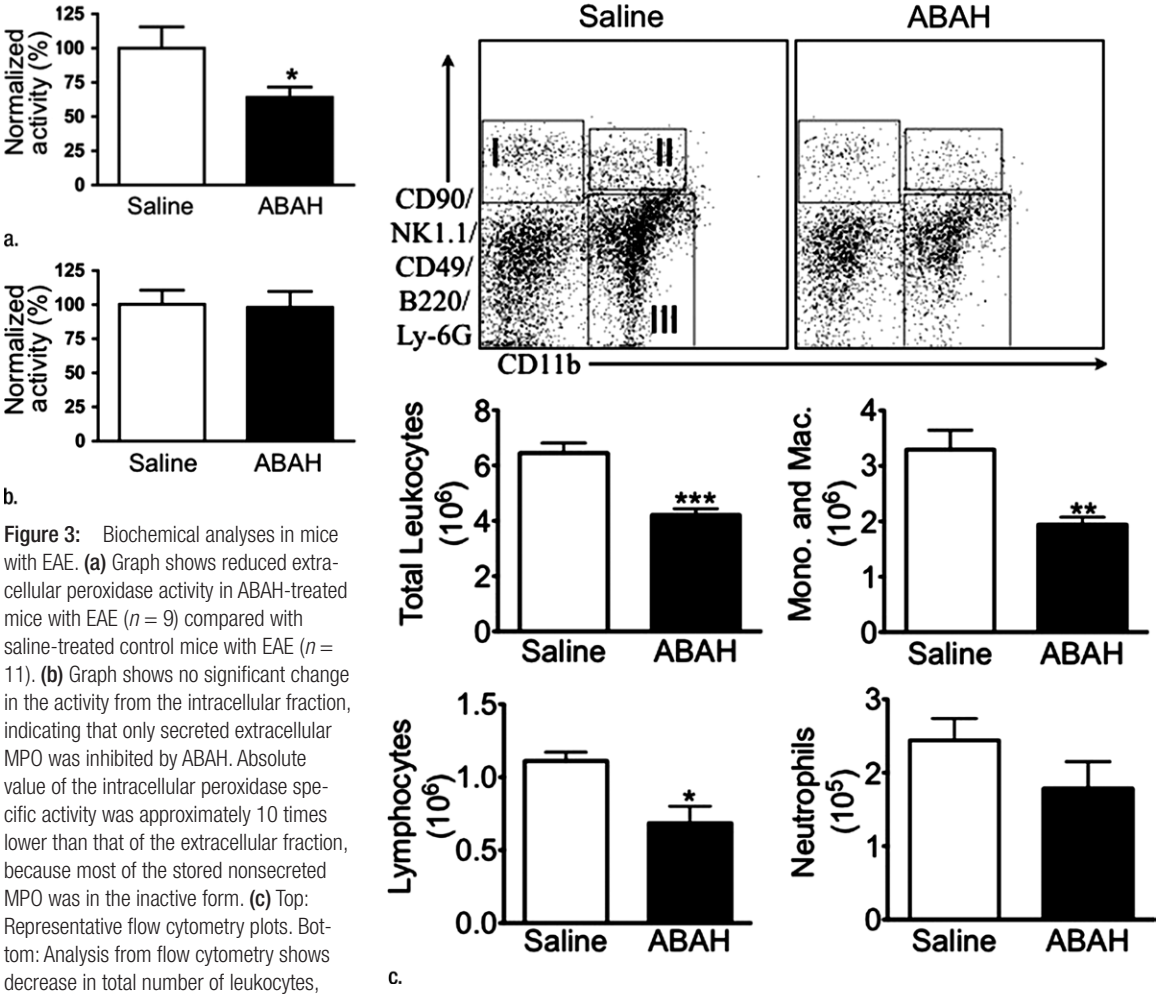

Figure 3: Biochemical analyses in mice with EAE. **(a)** Graph shows reduced extracellular peroxidase activity in ABAH-treated mice with EAE ($n = 9$) compared with saline-treated control mice with EAE ($n = 11$). **(b)** Graph shows no significant change in the activity from the intracellular fraction, indicating that only secreted extracellular MPO was inhibited by ABAH. Absolute value of the intracellular peroxidase specific activity was approximately 10 times lower than that of the extracellular fraction, because most of the stored nonsecreted MPO was in the inactive form. **(c)** Top: Representative flow cytometry plots. Bottom: Analysis from flow cytometry shows decrease in total number of leukocytes, including monocytes *(Mono.) and* macrophages and microglia *(Mac.)*, and lymphocytes in brains of ABAH-treated mice with EAE compared with saline-treated control mice with EAE ($n = 10$ per group). *I* = lymphocytes, *II* = neutrophils, *III* = monocytes/macrophages/microglia, $* = P < .05$, $** = P < .01$, $*** = P < .001$, error bars = standard error.

(36–39) and sensitivity (28,29,38,40) of MPO-Gd imaging in mouse and rabbit disease models, in MPO-deficient animals, and by comparing MPO-Gd with nonfunctional analogs and conventional gadolinium-based imaging agents (Appendix E1 [online]). In this study, by using a competitive irreversible inhibitor against MPO, we further showed that MPO-Gd molecular imaging could accurately depict the changes in MPO activity in vivo after treatment, matching in vitro tissue assay results. Therefore, MPO-Gd imaging could be used as an imaging biomarker to assess and follow disease activity in animal models of inflammatory demyelination, and potentially in human MS.

Our findings are concordant with multiple lines of evidence implicating macrophages and microglia and indirectly MPO activity as mediators of tissue damage in MS (1,3,7,17,41,42). However, it was previously observed that MPO-deficient mice with EAE had higher morbidity and mortality compared with their wild-type counterparts (23). While the cause of this difference is likely complex, in animals completely devoid of MPO there is likely developmental upregulation of compensatory inflammatory molecules with distinct biological functions from MPO that may explain the observed exacerbation in those mice. This concept is supported by increased proliferation of antigen-specific T cells in MPO-deficient mice with EAE (23). Furthermore, heterozygous MPO-deficient mice with EAE actually exhibited slightly improved symptoms compared with wild-type mice and did not demonstrate the deterioration in symptoms seen with homozygotes completely lacking MPO (23). These findings thus

Figure 4

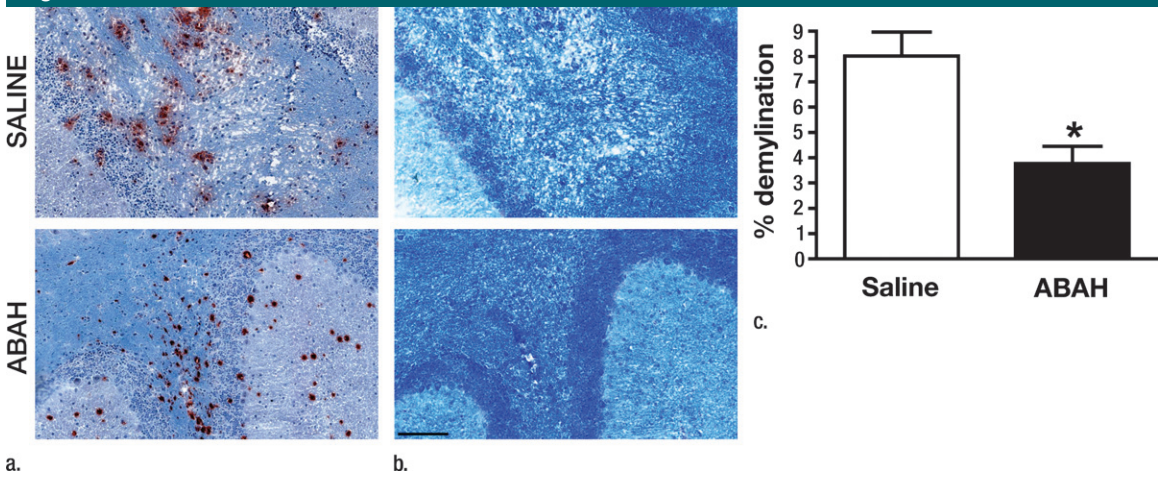

Figure 4: MPO inhibition results in decreased tissue damage and demyelination. **(a)** Immunohistochemical sections selected for areas with a similar degree of MPO-positive cell infiltration in saline-treated and ABAH-treated mice with EAE (MPO stain), but **(b)** adjacent sections demonstrate less demyelination in the ABAH-treated mice with EAE (Luxol fast blue stain). Bar = 50 μm. (Original magnification, ×400.) **(c)** Graph shows significantly less demyelination in ABAH-treated mice with EAE compared with saline-treated mice with EAE (six mice, three in each group, total of 27 sections evaluated). Mann-Whitney *U* test was used. ∗ = $P < .05$, error bars = standard error.

support our results that partial inhibition of MPO activity is beneficial.

MPO appears to be involved in positive feedback regulation of inflammation, as observed in both published literature (43–47) and our study. Indeed, investigators in a recent study found that MPO can bring together endothelial and leukocyte membranes via electrostatic forces (44), potentially acting as a positive feedback for cell recruitment. This is consistent with our observation of decreased inflammatory cell infiltration of the brain after MPO inhibition. The beneficial effects of MPO inhibition in EAE are thus the result of both directly reducing tissue-damaging substances and free radicals and indirectly decreasing inflammatory cell recruitment to the brain.

Our study had several limitations. First, while EAE is the most commonly used autoimmune animal model for MS, other animal models exist and may prove to be more reflective of the true MS pathogenesis. Cuprizone is the most commonly used toxin to induce demyelination in animals. The advantage of this model is the high reproducibility of the lesions. The major drawbacks of this model are that its disease pattern is distinct from human MS and the toxin is unrelated to MS. Theiler murine encephalomyelitis virus is the most commonly used infectious agent to induce demyelination. The chronic phase of Theiler murine encephalomyelitis virus is progressive rather than relapsing and remitting, as more commonly seen in the autoimmune model. Second, the high variability and a predominantly spinal cord distribution of the lesions is different from the widespread disease seen in most MS subtypes in the brain in addition to the spinal cord (41). Third, we administered ABAH daily, aiming to prevent neuroinflammation. It is possible that treatment after symptom onset may also be effective. Thus, we are planning studies with ABAH administration at different times of EAE disease evolution in the near future. Fourth, like all immunomodulatory therapies, MPO inhibition has the potential for immunologic side effects, particularly an increased susceptibility to infections. We did not observe any adverse effects or evidence of an increased susceptibility to infection, similar to the clinical experience with MPO-deficient humans (48). In addition to primarily targeting the myeloid-lineage inflammatory cells rather than lymphocytes, another aspect of MPO therapy is that MPO represents a downstream effector of the inflammatory cascade. This may decrease unwanted side effects that may arise from the more upstream inhibition of the immune system.

Our study suggests that MPO may be a key mediator of myeloid inflammation and tissue damage in EAE. Therefore, MPO could represent a promising therapeutic target, as well as an imaging biomarker for demyelinating diseases and potentially for other diseases in which MPO is implicated. Future development of more potent MPO inhibitors thus may be an attractive strategy for the treatment of inflammatory demyelinating diseases such as MS.

Disclosures of Potential Conflicts of Interest: **R.F.** Financial activities related to the present article: none to disclose. Financial activities not related to the present article: owns stocks and stock options in Real Time Radiology, a teleradiology company. Other relationships: none to disclose. **G.R.W.** No potential conflicts of interest to disclose. **Y.Z.** No potential conflicts of interest to disclose. **D.S.** No potential conflicts of interest to disclose. **B.R.M.B.** No potential conflicts of interest to disclose. **B.P.** No potential conflicts of interest to disclose. **A.R.M.** No potential conflicts of interest to disclose. **W.L.A.** No potential conflicts of interest to disclose. **Y.I.** No potential conflicts of interest to disclose. **E.R.Z.** No potential conflicts of interest to disclose. **M.E.** No potential conflicts of interest to disclose. **E.R.** No potential conflicts of

Figure 5

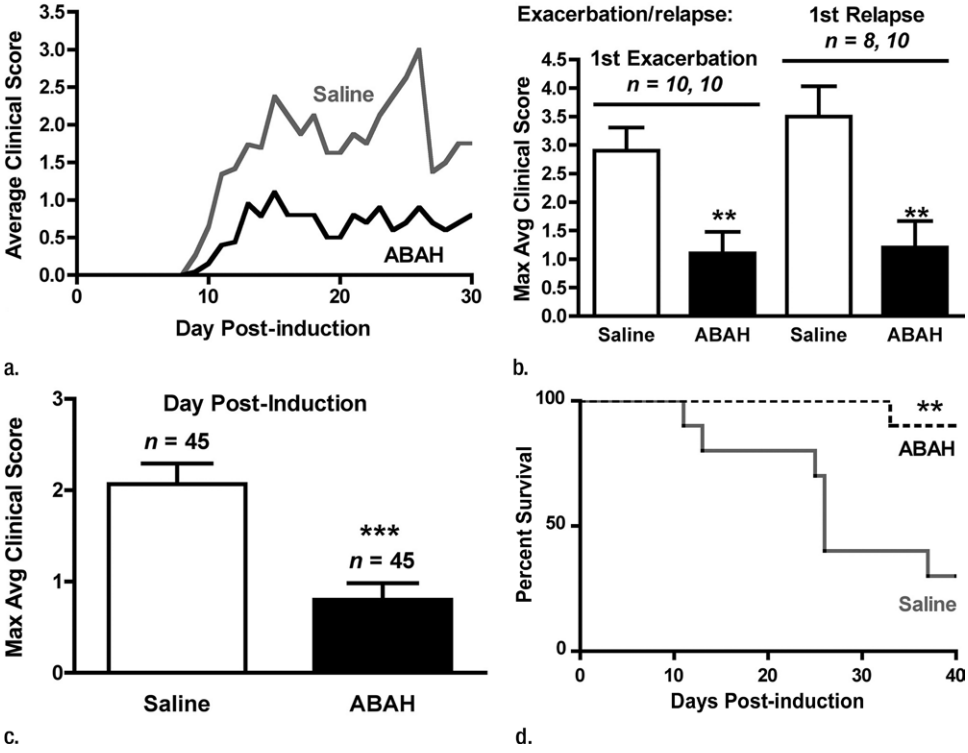

Figure 5: Graphs show that MPO inhibition improves clinical symptoms and survival of mice with EAE. **(a)** Average clinical scores from 45 control saline-treated and 45 ABAH-treated mice with EAE demonstrate reduced disease exacerbation. **(b)** Significantly decreased maximum average clinical score was observed in the treated group during the first exacerbation and first relapse (10 saline-treated mice, 10 ABAH-treated mice) followed up to day 40. Error bars = standard error. **(c)** Maximum average clinical score in all 90 mice is also significantly decreased in the ABAH-treated group. Because some mice were analyzed before peak clinical disease, the average scores were slightly lower than shown in **b**. Error bars = standard error. **(d)** Of 20 mice followed up to day 40, only three of 10 control mice survived to day 40 compared with nine of 10 in the treated group. Additional information is provided in Figure E2 (online). ** = $P < .01$, *** = $P < .001$.

interest to disclose. **C.S.R.** No potential conflicts of interest to disclose. **F.K.S.** No potential conflicts of interest to disclose. **R.W.** No potential conflicts of interest to disclose. **J.W.C.** Financial activities related to the present article: institution received a grant from the Dana Foundation. Financial activities not related to the present article: institution received a grant from Pfizer, author receives royalties for a textbook from Elsevier. Other relationships: none to disclose.

References

1. Gray E, Thomas TL, Betmouni S, Scolding N, Love S. Elevated myeloperoxidase activity in white matter in multiple sclerosis. Neurosci Lett 2008;444(2):195–198.
2. Gray E, Thomas TL, Betmouni S, Scolding N, Love S. Elevated activity and microglial expression of myeloperoxidase in demyelinated cerebral cortex in multiple sclerosis. Brain Pathol 2008;18(1):86–95.
3. Heppner FL, Greter M, Marino D, et al. Experimental autoimmune encephalomyelitis repressed by microglial paralysis. Nat Med 2005;11(2):146–152.
4. Bartnik BL, Juurlink BH, Devon RM. Macrophages: their myelinotrophic or neurotoxic actions depend upon tissue oxidative stress. Mult Scler 2000;6(1):37–42.
5. Jack C, Ruffini F, Bar-Or A, Antel JP. Microglia and multiple sclerosis. J Neurosci Res 2005;81(3):363–373.
6. Noseworthy JH, Lucchinetti C, Rodriguez M, Weinshenker BG. Multiple sclerosis. N Engl J Med 2000;343(13):938–952.
7. Rasmussen S, Wang Y, Kivisäkk P, et al. Persistent activation of microglia is associated with neuronal dysfunction of callosal projecting pathways and multiple sclerosis-like lesions in relapsing–remitting experimental autoimmune encephalomyelitis. Brain 2007;130(pt 11):2816–2829.
8. Barnett MH, Prineas JW. Relapsing and remitting multiple sclerosis: pathology of the newly forming lesion. Ann Neurol 2004;55(4):458–468.
9. Kutzelnigg A, Lucchinetti CF, Stadelmann C, et al. Cortical demyelination and diffuse white matter injury in multiple sclerosis. Brain 2005;128(pt 11):2705–2712.
10. Randomised double-blind placebo-controlled study of interferon beta-1a in relapsing/remitting multiple sclerosis. PRISMS (Prevention of Relapses and Disability by Interferon beta-1a Subcutaneously in Multiple Sclerosis) Study Group. Lancet 1998;352(9139):1498–1504.
11. Placebo-controlled multicentre randomised trial of interferon beta-1b in treatment of secondary progressive multiple sclerosis. European Study Group on interferon beta-1b in secondary progressive MS. Lancet 1998;352(9139):1491–1497.

12. Axtell RC, de Jong BA, Boniface K, et al. T helper type 1 and 17 cells determine efficacy of interferon-beta in multiple sclerosis and experimental encephalomyelitis. Nat Med 2010;16(4):406–412.

13. Jacobs LD, Beck RW, Simon JH, et al. Intramuscular interferon beta-1a therapy initiated during a first demyelinating event in multiple sclerosis. CHAMPS Study Group. N Engl J Med 2000;343(13):898–904.

14. Johnson KP, Brooks BR, Cohen JA, et al. Copolymer 1 reduces relapse rate and improves disability in relapsing-remitting multiple sclerosis: results of a phase III multicenter, double-blind placebo-controlled trial. The Copolymer 1 Multiple Sclerosis Study Group. Neurology 1995;45(7):1268–1276.

15. Polman CH, O'Connor PW, Havrdova E, et al. A randomized, placebo-controlled trial of natalizumab for relapsing multiple sclerosis. N Engl J Med 2006;354(9):899–910.

16. Bradley PP, Christensen RD, Rothstein G. Cellular and extracellular myeloperoxidase in pyogenic inflammation. Blood 1982;60(3):618–622.

17. Nagra RM, Becher B, Tourtellotte WW, et al. Immunohistochemical and genetic evidence of myeloperoxidase involvement in multiple sclerosis. J Neuroimmunol 1997;78(1-2):97–107.

18. Heinecke JW. Tyrosyl radical production by myeloperoxidase: a phagocyte pathway for lipid peroxidation and dityrosine cross-linking of proteins. Toxicology 2002;177(1):11–22.

19. Zhang R, Brennan ML, Shen Z, et al. Myeloperoxidase functions as a major enzymatic catalyst for initiation of lipid peroxidation at sites of inflammation. J Biol Chem 2002;277(48):46116–46122.

20. Eiserich JP, Baldus S, Brennan ML, et al. Myeloperoxidase, a leukocyte-derived vascular NO oxidase. Science 2002;296(5577):2391–2394.

21. Galijasevic S, Saed GM, Diamond MP, Abu-Soud HM. Myeloperoxidase up-regulates the catalytic activity of inducible nitric oxide synthase by preventing nitric oxide feedback inhibition. Proc Natl Acad Sci U S A 2003;100(25):14766–14771.

22. Wang Z, Nicholls SJ, Rodriguez ER, et al. Protein carbamylation links inflammation, smoking, uremia and atherogenesis. Nat Med 2007;13(10):1176–1184.

23. Brennan M, Gaur A, Pahuja A, Lusis AJ, Reynolds WF. Mice lacking myeloperoxidase are more susceptible to experimental autoimmune encephalomyelitis. J Neuroimmunol 2001;112(1-2):97–105.

24. Chataway J, Sawcer S, Feakes R, et al. A screen of candidates from peaks of linkage: evidence for the involvement of myeloperoxidase in multiple sclerosis. J Neuroimmunol 1999;98(2):208–213.

25. Nelissen I, Fiten P, Vandenbroeck K, et al. PECAM1, MPO and PRKAR1A at chromosome 17q21-q24 and susceptibility for multiple sclerosis in Sweden and Sardinia. J Neuroimmunol 2000;108(1-2):153–159.

26. Zakrzewska-Pniewska B, Styczynska M, Podlecka A, et al. Association of apolipoprotein E and myeloperoxidase genotypes to clinical course of familial and sporadic multiple sclerosis. Mult Scler 2004;10(3):266–271.

27. Ramsaransing G, Teelken A, Prokopenko VM, Arutjunyan AV, De Keyser J. Low leucocyte myeloperoxidase activity in patients with multiple sclerosis. J Neurol Neurosurg Psychiatry 2003;74(7):953–955.

28. Chen JW, Breckwoldt MO, Aikawa E, Chiang G, Weissleder R. Myeloperoxidase-targeted imaging of active inflammatory lesions in murine experimental autoimmune encephalomyelitis. Brain 2008;131(pt 4):1123–1133.

29. Chen JW, Querol Sans M, Bogdanov A Jr, Weissleder R. Imaging of myeloperoxidase in mice by using novel amplifiable paramagnetic substrates. Radiology 2006;240(2):473–481.

30. Kettle AJ, Gedye CA, Hampton MB, Winterbourn CC. Inhibition of myeloperoxidase by benzoic acid hydrazides. Biochem J 1995;308(pt 2):559–563.

31. Kettle AJ, Gedye CA, Winterbourn CC. Mechanism of inactivation of myeloperoxidase by 4-aminobenzoic acid hydrazide. Biochem J 1997;321(pt 2):503–508.

32. Malle E, Furtmüller PG, Sattler W, Obinger C. Myeloperoxidase: a target for new drug development? Br J Pharmacol 2007;152(6):838–854.

33. de Haas AH, Boddeke HW, Brouwer N, Biber K. Optimized isolation enables ex vivo analysis of microglia from various central nervous system regions. Glia 2007;55(13):1374–1384.

34. Klebanoff SJ, Waltersdorph AM, Rosen H. Antimicrobial activity of myeloperoxidase. Methods Enzymol 1984;105:399–403.

35. Shashoua VE. Extracellular fluid proteins of goldfish brain: studies of concentration and labeling patterns. Neurochem Res 1981;6(10):1129–1147.

36. Breckwoldt MO, Chen JW, Stangenberg L, et al. Tracking the inflammatory response in stroke in vivo by sensing the enzyme myeloperoxidase. Proc Natl Acad Sci U S A 2008;105(47):18584–18589.

37. Rodríguez E, Nilges M, Weissleder R, Chen JW. Activatable magnetic resonance imaging agents for myeloperoxidase sensing: mechanism of activation, stability, and toxicity. J Am Chem Soc 2010;132(1):168–177.

38. Nahrendorf M, Sosnovik D, Chen JW, et al. Activatable magnetic resonance imaging agent reports myeloperoxidase activity in healing infarcts and noninvasively detects the antiinflammatory effects of atorvastatin on ischemia-reperfusion injury. Circulation 2008;117(9):1153–1160.

39. Swirski FK, Wildgruber M, Ueno T, et al. Myeloperoxidase-rich Ly-6C+ myeloid cells infiltrate allografts and contribute to an imaging signature of organ rejection in mice. J Clin Invest 2010;120(7):2627–2634.

40. Ronald JA, Chen JW, Chen Y, et al. Enzyme-sensitive magnetic resonance imaging targeting myeloperoxidase identifies active inflammation in experimental rabbit atherosclerotic plaques. Circulation 2009;120(7):592–599.

41. Rivest S. Regulation of innate immune responses in the brain. Nat Rev Immunol 2009;9(6):429–439.

42. Bauer J, Sminia T, Wouterlood FG, Dijkstra CD. Phagocytic activity of macrophages and microglial cells during the course of acute and chronic relapsing experimental autoimmune encephalomyelitis. J Neurosci Res 1994;38(4):365–375.

43. Gelderman MP, Stuart R, Vigerust D, et al. Perpetuation of inflammation associated with experimental arthritis: the role of macrophage activation by neutrophilic myeloperoxidase. Mediators Inflamm 1998;7(6):381–389.

44. Klinke A, Nussbaum C, Kubala L, et al. Myeloperoxidase attracts neutrophils by physical forces. Blood 2011;117(4):1350–1358.

45. Lau D, Mollnau H, Eiserich JP, et al. Myeloperoxidase mediates neutrophil activation by association with CD11b/CD18 integrins. Proc Natl Acad Sci U S A 2005;102(2):431–436.

46. Lefkowitz DL, Mills K, Morgan D, Lefkowitz SS. Macrophage activation and immunomodulation by myeloperoxidase. Proc Soc Exp Biol Med 1992;199(2):204–210.

47. Shepherd VL, Hoidal JR. Clearance of neutrophil-derived myeloperoxidase by the macrophage mannose receptor. Am J Respir Cell Mol Biol 1990;2(4):335–340.

48. Lanza F. Clinical manifestation of myeloperoxidase deficiency. J Mol Med (Berl) 1998;76(10):676–681.